

Provided for non-commercial research and education use.  
Not for reproduction, distribution or commercial use.



This article appeared in a journal published by Elsevier. The attached copy is furnished to the author for internal non-commercial research and education use, including for instruction at the authors institution and sharing with colleagues.

Other uses, including reproduction and distribution, or selling or licensing copies, or posting to personal, institutional or third party websites are prohibited.

In most cases authors are permitted to post their version of the article (e.g. in Word or Tex form) to their personal website or institutional repository. Authors requiring further information regarding Elsevier's archiving and manuscript policies are encouraged to visit:

<http://www.elsevier.com/copyright>



Contents lists available at ScienceDirect

## Composites: Part A

journal homepage: [www.elsevier.com/locate/compositesa](http://www.elsevier.com/locate/compositesa)

# Ferromagnetic microwires enabled polymer composites for sensing applications

Faxiang Qin<sup>a,\*</sup>, Hua-Xin Peng<sup>a</sup>, Jie Tang<sup>b</sup>, Lu-Chang Qin<sup>c</sup>

<sup>a</sup>Advanced Composite Center for Innovation and Science, Department of Aerospace Engineering, University of Bristol, University Walk, Bristol BS8 1TR, UK

<sup>b</sup>1D Nanomaterials Research Group, National Institute for Materials Science, Sengen 1-2-1, Tsukuba 305-0042, Japan

<sup>c</sup>W.M. Keck Laboratory for Atomic Imaging and Manipulation, Department of Physics and Astronomy, University of North Carolina at Chapel Hill, Chapel Hill, NC 27599-3255, USA

## ARTICLE INFO

### Article history:

Received 21 April 2010

Received in revised form 9 September 2010

Accepted 10 September 2010

### Keywords:

B. Magnetic properties

A. Smart materials

## ABSTRACT

In the present work, sensing functionalities are introduced into structural composites via embedded magnetic microwires. A systematic study on the structure and functionalities of microwires and their composites is performed. The single-wire composite shows a significant giant magnetoimpedance (GMI) effect of up to 320% in a frequency range of 1–100 MHz due to stress enhanced transverse magneto-anisotropy. With increasing quantities of embedded wires from 1 to 3, the maximum GMI ratio is enhanced significantly by more than 35%, making the resultant composite favourable for field sensing applications. The microwire-composite also shows superior stress-sensing resolution as high as 134.5 kHz/microstrain, which is about 26 times higher than the recently proposed SRR-based sensor. As evidenced by the structural examination and tensile tests, the extremely small volume fraction of microwires (~0.01 vol.%) allows the wire-composites to retain their mechanical integrity and performance.

© 2010 Elsevier Ltd. All rights reserved.

## 1. Introduction

A multi-functional composite essentially refers to a composite material that, beyond the primary structural function, possesses other functionalities as well achieved by constituent materials in an optimized structure [1,2]. Therefore, two points are highlighted in this definition: (i) the composite must have multiple functions, and (ii) the additional functions are enabled by the constitutive elements in the material. Such a concept has led us to target the efforts into exploring ideal functional fillers that could meet the criteria: (i) a likely omnipotent functional filler that will ensure the achievement of multi-functionalities and a relatively simple composite architecture, and (ii) preferred fine geometry and large susceptibility to external fields to warrant a low and effective loading of fillers that enables a homogeneous material in favour of structural integrity and implementation. In this context, microwires embedded in a polymeric matrix can meet the above criteria.

Co-based glass-coated microwires (AGCMs) have a unique circular magnetic anisotropy due to coupling between the negative magnetostriction and frozen-in stress. Such anisotropy is important to realise a large and sensitive magnetoimpedance (MI) effect for applications in miniature magnetic sensors and sensing composite media [3]. The MI effect refers to a strong variation in the electrical impedance of a magnetic conductor subject to a small

dc magnetic field, which is observed at frequencies when the skin effect is strong. Based on the frequency range, it can be classified into three regions [4–8]: (i) at a relatively low-frequency range of a few 100 kHz–MHz, the change of impedance is mainly due to circular domain wall dynamics; (ii) at the intermediate frequency range from a few MHz to a few 100 MHz, the domain wall motion is strongly damped and the rotational processes mainly contribute to the ac permeability and impedance change; (iii) at frequencies of the GHz range where ferromagnetic resonance (FMR) occurs, the rotational permeability becomes less sensitive to the field and the impedance change is related to FMR. In all three cases, the characteristic field of the impedance change is defined by the value and distribution of the circular anisotropy. Since the discovery of GMI in 1994 [9], a variety of ferromagnetic materials including amorphous ribbons [10–13], microwires [14–18], composite wires [19,20], and thin films [21–23], have been investigated for the purpose of improving the GMI effect through proper treatment and developing new magnetic materials with the best possible GMI performance.

In this work, a ferromagnetic/dielectric heterogeneous composite with embedded amorphous glass-coated microwires (AGCMs) in the E-glass prepreg matrix is proposed. The polymer matrix, glass-coating layer, and metallic core allow more freedoms in manipulating the properties of the resultant composites. After curing under controlled temperature and pressure, AGCMs as the sensing elements and the matrix as the dielectric media yield an excellent GMI performance. The superior stress-sensing capability of the proposed composite is also demonstrated analytically.

\* Corresponding author.

E-mail address: [faxiang.qin@bristol.ac.uk](mailto:faxiang.qin@bristol.ac.uk) (F. Qin).

## 2. Experimental

Soft magnetic glass-coated microwires  $\text{Co}_{68.7}\text{Fe}_4\text{Ni}_1\text{B}_{13}\text{Si}_{11}\text{Mo}_{2.3}$  were fabricated by a modified Taylor-Ulitovskiy method [24,25]. These microwires (supplied by MFTI, Moldova) consist of a metallic core of diameter  $17.6\ \mu\text{m}$  and a glass coat of thickness  $3.3\ \mu\text{m}$ , as shown in Fig. 1. Scanning electron microscopes (SEM, (i) HITACHI S-5500 & (ii) JEOL JSM-6500) were used for examining the wires. The corresponding SEM specimens were prepared by (i) cross-section polishing of the wires and (ii) mechanical polishing of the wire-embedded resin stubs, respectively. The acceleration voltage was set to 15 kV for all SEM examinations. The microwires possess good soft magnetic properties owing to the vanishing magnetostriction ( $\sim -10^{-7}$ ) and are suitable for megahertz operations. The microwire composites were prepared by embedding microwires into a 913 E-glass prepreg matrix in a parallel manner. First, the microwire(s) were laid out at zero degree along the glass-fibre direction between the two layers of prepreps. Two additional layers were laid on the top and the bottom of the microwire-embedded layers in the same direction, resulting in a layup of four prepreg layers with the continuous wires in the middle. The composite was then sent to an autoclave for curing as detailed elsewhere [26]. (LM) ZEISS JENA VERT optical microscope was used for examining the surface morphology of prepared composites.

The electrical impedance was measured using a HP8753E network analyser in the frequency range of 1–100 MHz. The composite sample of in-plane size  $10\ \text{mm} \times 10\ \text{mm}$  was set in the measurement cell subject to a DC magnetic field of up to  $30\ \text{Oe}$  along the wire axis and vertical to the geomagnetic field. The S11 port of the two-port network was used to pick up the signals of output power and the S-parameter was then converted to the impedance through a computer program. The magnetoimpedance ratio  $\Delta Z/Z$  is defined as

$$\frac{\Delta Z}{Z} (\%) = \frac{Z(H) - Z(H_{\max})}{Z(H_{\max})} \times 100\%, \quad (1)$$

where  $Z(H)$  and  $Z(H_{\max})$  are the magnetic impedance value of the sample in the external magnetic field  $H$  and the maximum magnetic field  $H_{\max}$  to saturate the impedance, respectively. The field sensitivity  $\xi$  is defined as the slope of the variation of magnetoimpedance ratio (MIR) with an external magnetic field at the vicinity of zero field, which is expressed as [27]:

$$\xi = \left[ \frac{(\Delta Z/Z)}{H} \right]_{H \rightarrow 0}. \quad (2)$$

The mechanical properties of the wire-composites were measured using an INSTRON tensile tester with a load capacity of 30 kN. Three sets of testing coupons including blank composites, ten-continuous-wire composites and fifty-short-wire composites

with the identical size of  $160 \times 26 \times 0.65\ \text{mm}^3$  were prepared by gluing tabs on both ends using Redux 810A/B. At least 4 specimens were tested for each set of samples and the tests showed good consistency.

## 3. Results and discussion

### 3.1. Structural characterisation

The basic structure of the microwires is illustrated in Fig. 1a, whereby the metallic core (I) is covered by glass-coat (II). A closer inspection on interfacial structure between the core and the coat layer is illustrated in Fig. 1b. A typical observed region shows that the glass coat and the metallic core are partially bonded and partially disconnected by surface cracks (indicated by an arrow in the figure) occurred to the glass. This exemplifies the interfacial conditions of the fine microwires fabricated by the Taylor-Ulitovskiy method, suggesting that such a discontinuous surface may result in an intricate influence on the magnetic domain configuration of microwires. This explains the falling-off of very thin glass layers sometimes during the manual handling of the samples.

An in-plane optical micrograph of the prepared composite is shown in Fig. 2a. On the exterior surface, one can see several ridges of different colours than other regions (indicated by arrows), which is attributed to a non-uniform distribution of the resin and glass-fibre in the prepreps [28], as revealed in the scanning electron microscope (SEM) image of the cross-section (Fig. 2b). It is the microwire, which is slightly thicker than the glass-fibres, that causes the non-uniform distribution of the resin in the region close to it. However, such influence from the microwires is limited to the near-wire region only and is comparable to the inherent defects in the prepreps. In addition, since the microwire-composite is intended to contain a very small number of wires that are separated in a spacing of a few millimetres to a few centimetres, which is 3–4 orders of magnitude larger than the diameter of the microwires, the disruption of microwires to the composite integrity is minimal. This is further confirmed by an examination of the mechanical properties discussed in Section 3.4.

It should be noted that the residual stresses between the glass-coat and the metallic core are compounded by the resin covering the microwire and the glass fibres in nearest-neighbour. Therefore, since the coefficient of thermal expansion of the epoxy resin ( $\sim 10^{-6}$ ) is one order of magnitude higher than that of the glass, the imposed stress on the microwire is expected to increase. This will yield an increase of the magnetoelastic anisotropy energy in the transverse direction with respect to the wire axis. As a result, transverse coercivity is decreased and permeability is increased [29,30]. This leads to an enhanced GMI effect owing to the incorporation of the microwires.

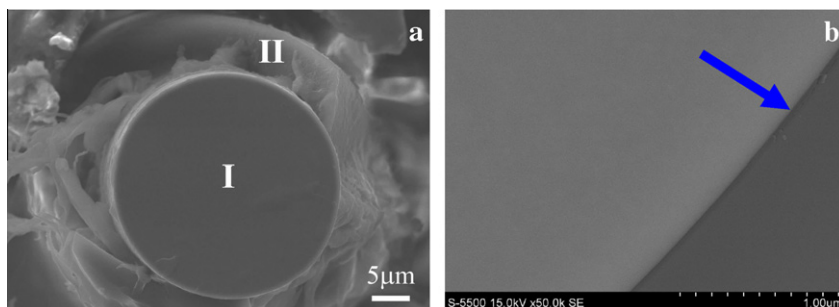
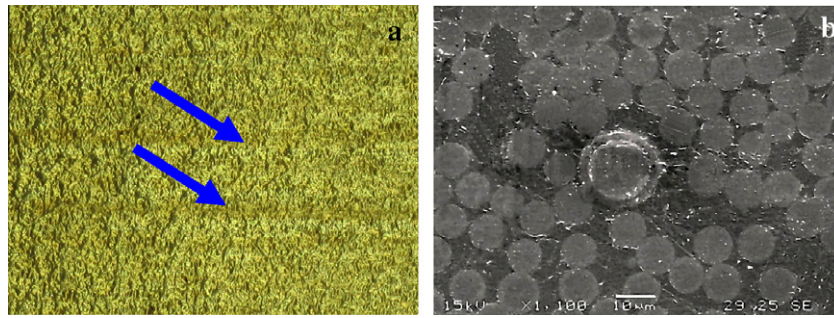


Fig. 1. Cross-sectional SEM images of glass-coated  $\text{Co}_{68.7}\text{Fe}_4\text{Ni}_1\text{B}_{13}\text{Si}_{11}\text{Mo}_{2.3}$  microwire. (a) SEM image showing the metal core (I) and glass coating (II). (b) Cracks in the interfacial region between the metal core and the glass coating.



**Fig. 2.** (a) In-plane view optical micrographs of the composite surface and (b) a cross-sectional SEM image of the composite where both the single metal microwire with glass coating and glass fibres in the composite are shown.

### 3.2. Field sensing

Results on the GMI of the composites containing a single microwire in the frequency range of 1–100 MHz are given in Fig. 3a. The MI effect is increased with increasing frequency ( $f$ ). At  $f = 1$  MHz, the MI effect is so weak that it would be insignificant from the viewpoint of applications. This weak MI effect is attributed to the weak dependence of the imaginary part of the impedance on the frequency, thereby resulting in an absolute value of the impedance close to the dc resistance of the microwire. The underlying mechanism lies in the weak interactions between the ac field induced by the ac current and the applied dc magnetic field, which is supposed to govern the GMI effect. When the frequency reaches 30 MHz, the MI ratio (MIR) and sensitivity become 126% and 11.6%/Oe, respectively. Actually the GMI effect starts to occur at this frequency because the MIR exceeds 100% [31]. At frequency up to 100 MHz, the MIR and sensitivity are increased to 320% and 30%/Oe, respectively. It should be noted that, in the measured frequency range, the GMI profiles remain a double peak feature, which indicates the magnetization process dominated by the spin rotation rather

than the domain wall displacement. The monotonous increase of maximum GMI value with the frequency (Fig. 4a), in response to the magnetization by spin rotation, is caused by an enhancement of the skin effect with increasing frequency. In comparison with amorphous ribbons [9,32], the microwire-composites do not display any peak value of maximum GMI corresponding to the characteristic frequency in the frequency range of 1–100 MHz, implying that the characteristic frequency shifts to a higher frequency value [33]. This feature is favourable for the high-frequency sensing applications.

Subsequently, we examined the frequency dependence of the field at which the GMI reaches the maximum value, i.e., the anisotropy field. It can be seen from Fig. 4a that the anisotropy field shows a similar trend against frequency as the maximum GMI does. This can be understood with the aid of the domain model and eddy-current model. According to the domain model [32], the improvement of GMI is due to the increase of circumferential permeability, which is resulted from the approaching of anisotropic direction to the circumferential field. Therefore, the anisotropy field increases with a better-defined anisotropy [33]. The

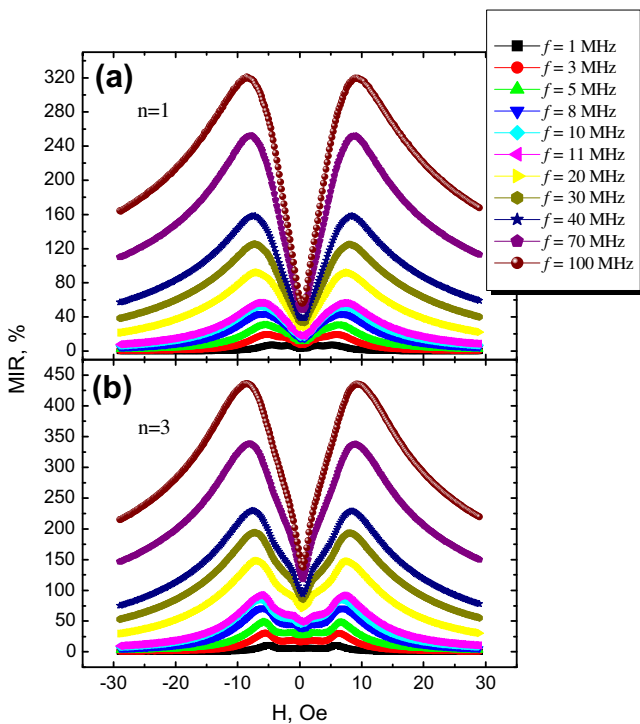


**Fig. 3.** Axial field dependence of GMI profiles of composites containing (a) single wire and (b) three wires at different frequencies.

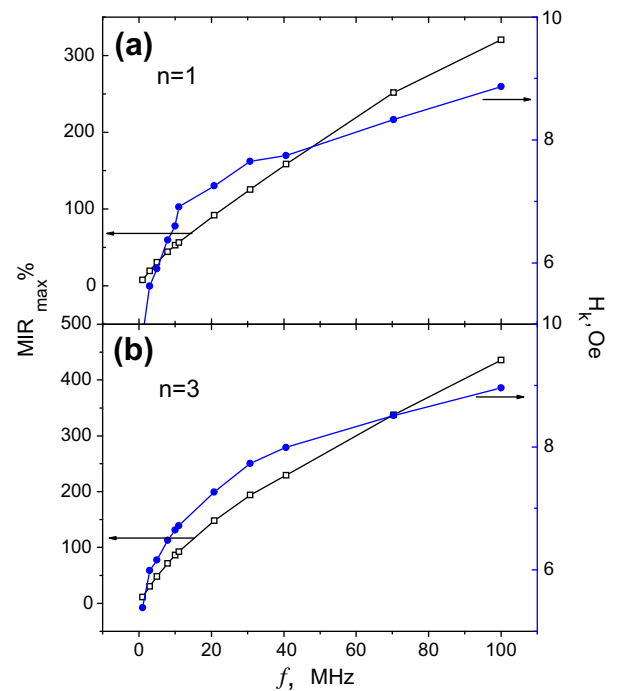


**Fig. 4.** Frequency dependence of the maximum GMI value and the anisotropy field determined from GMI profiles for composite incorporating (a) single wire and (b) three wires.

skin effect based on regional magnetoelastic anisotropy is responsible for this feature according to eddy-current model. Essentially, the increase of frequency will enhance the skin effect by diminishing the skin depth, resulting in inhomogeneity of current distribution, which concentrates in the region close to the surface. It should also be noted that a knee (Fig. 4a) is observed on the curve at 10 MHz, indicating that the anisotropy energy is less influenced at higher frequencies. In short, the composite will yield a larger GMI at higher frequencies but with a minor increase of energy loss, which is desirable for sensing applications.

Fig. 3b displays the GMI profiles of the composites containing multiple (three) wires in a parallel manner. In comparison with those single-wire composites, a conspicuous improvement of GMI effect was attained in the examined frequency range. The GMI effect starts at  $f = 5$  MHz with maximum MIR of 145% and sensitivity of 8.56%/Oe. At  $f = 100$  MHz, the maximum MIR and the sensitivity increased by over 30% and 50%, respectively, compared with those of the single-wire composite. The pronounced improvement of maximum MI effect can be understood by comparing the effective magnetic structure of the multi-wire and single-wire media in the presence of a magnetic field. The multiple wires in a parallel manner constitute an increase of the total cross-sectional area of the wires, resulting in a diminution of the effective ac resistivity and hence a stronger skin effect. Consequently the GMI effect is improved. In addition, the interactions of wires in the multi-wire composites induced magnetic closure to approach a more stable structure with the total energy decreased [34]. This leads to an increase of permeability and GMI effect. As also shown in Fig. 4b, the maximum GMI value and anisotropy field extracted from the GMI profiles of both composites exhibit a similar trend with increasing frequency, indicating the consistency of the GMI features in this kind of composites, which warrants the predictability for their applications.

### 3.3. Stress sensing

Following the low-field GMI phenomena utilized for field sensing, this section is focused on the high field absorption that can be potentially used for stress sensing. Here we treated theoretically the GMI phenomenon in the microwave frequency range ( $\sim$ GHz) by analysing the ferromagnetic resonance (FMR), which is considered to be related to the high-frequency GMI. Using the classic Landau–Lifschitz–Gilbert equation, in the case of ferromagnetic wires or composite containing arrays of wires, one can obtain Eq. (3) to calculate the variation of the imaginary component of permeability with varying applied magnetic fields[35]:

$$\mu = 1 + \frac{\mu_0 \gamma M_s [\mu_0 \gamma (H_{dc} + H_k) - j\omega\alpha]}{-\omega^2 + \omega_{FMR}^2 - j\omega\alpha\mu_0 \gamma [2(H_{dc} + H_k) + M_s]}, \quad (3)$$

where  $\mu_0$  is the vacuum permeability,  $\alpha$  is the damping parameter,  $\gamma$  is the gyromagnetic parameter,  $M_s$  is the saturation magnetization,  $H_{dc}$  denotes the applied magnetic field,  $H_k$  is the anisotropy field,  $\omega$  is the angular frequency and  $\omega_{FMR}$  denotes the angular resonance frequency which is given by[36]

$$\omega_{FMR} = \mu_0 \gamma \sqrt{(H_{dc} + H_k + M_s)(H_{dc} + H_k)}. \quad (4)$$

It is reasonable to infer that, in addition to the magnetic field, stresses also produce a similar effect by modifying the magnetoelastic anisotropy of the microwires as expressed in Eq. (5) [37,38].

$$H_k = \frac{3|\lambda_s|}{M_s} (\sigma_{zz} - \sigma_{\phi\phi} + \sigma_{app}), \quad (5)$$

where  $\lambda_s$  is the magnetostriction constant ( $-10^{-7}$ ),  $M_s$  is the saturation magnetization,  $\sigma_{zz}$ ,  $\sigma_{\phi\phi}$  and  $\sigma_{app}$  are the longitudinal internal stress, radial internal stress, and applied stress, respectively. Insofar

as the microwire-composite architecture and curing conditions are unchanged, the internal stress is dependent on the geometry of the microwire, while the magnetostriction constant is mainly determined by the composition of the wires. Thus, the anisotropy field can be approximated as a linear function of the applied stress [39,40]. Using the numerical values of the relevant parameters for the studied wires, the stress tunable absorption spectra have been obtained as shown in Fig. 5a. Although the magnitude of absorption intensity varies with the number of wires, the resonance frequency

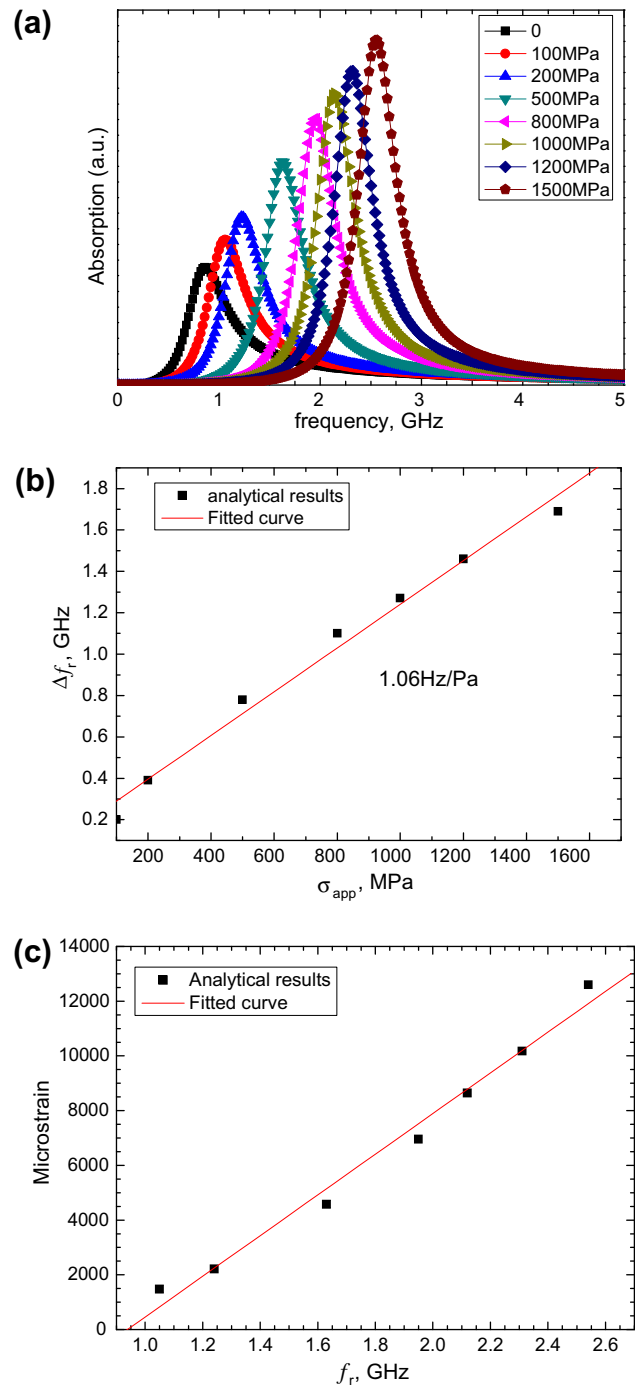


Fig. 5. (a) Calculated permeability spectra under varying  $\sigma_{app}$  according to Eqs. (3) and (5) with the material parameters obtained from magnetization test:  $M_s = 10^6$  A/m,  $\gamma = 2.21 \times 10^5$  mA $^{-1}$  s $^{-1}$ ,  $\alpha = 0.02$ ,  $H_k = 880$  A/m and  $\mu_0 = 1$ . (b) Applied stress dependence of resonance frequency shift. The slope of fitted line represents the stress-sensing resolution. (c) Resonance frequency dependence of microstrain. The slope of fitted line represents the strain sensing resolution.

**Table 1**

The mean values and coefficients of variation (CV\*) of Young's modulus and tensile strength for each set of samples.

Samples	Blank sample	10-wire sample	50-wire sample
<i>Properties</i>			
Young's modulus (GPa)	14.22 (3.1*)	14.48 (1.1)	14.97(3.0)
Tensile strength (MPa)	951.48 (6.3)	935.18(5.6)	1003.80 (3.8)

remains unchanged [41]. Therefore, this effect could be utilised for, beyond stress sensing, detecting and locating damages in the micro-wire-based composites [42], which is of much interest in engineering applications. In Figs. 5b and c, the sensing resolution is obtained from the shift of resonance with stress/strain with values of 1.06 MHz/MPa and 134.5 kHz/microstrain, respectively. These results lead to an important revelation that the microwires can be used as stress sensors in a wide frequency range provided the permeability can be obtained. Compared to the newly proposed SRR-based sensor with a sensitivity of 5.148 kHz/microstrain [43], the microwires are much more cost-effective and possess a higher *Q* factor and sensitivity. The susceptibility of permeability to stress can be largely tailored by either tuning the composition, geometry, and microstructure of the microwires [40] or through developing composites containing magnetic fillers [44] and non-magnetic fillers [45].

#### 3.4. Mechanical properties evaluation

As is known, when functional fillers such as optical fibres are introduced into a structural composite to enable additional functionalities, one major concern is the potential degradation of the mechanical performance caused by these fillers [46]. As such, we investigated the influence of the wires on the mechanical integrity of the resultant composites. From the stress–strain curves obtained for blank samples, 10-wire, and 50-wire samples under a maximum force of 30 kN, the Young's modulus and the tensile strength are summarised in Table 1. We observe that all the mechanical parameters are very close to each other for the different types of samples. In terms of the Young's modulus, the coefficient of variation (CV) for each type of samples is 3.1, 1.1 and 3.0. Upon performing cross comparison of their average properties, the CV is 2.6. Thus, these tensile testing results in conjunction with former structural examinations lead to the conclusion that the microwires embedded into the polymer matrix retained the mechanical performance of the original composite.

#### 4. Conclusions

The microwire-composites exhibit excellent GMI effect controllable via extremely small loading of microwire fillers, which is desirable for the sensing application. An enhanced GMI performance was obtained in the multi-wire composites through the interactions of the microwires in the presence of external magnetic field. The exceptional stress sensing function was analytically demonstrated. All these results will open up applications of the ferromagnetic/dielectric heterostructural composites as superior GMI-based field/stress sensors. It is also worth mentioning that such kind of microwire-composites also possess superior microwave tunable properties as elucidated in our previous work [38] and EMI shielding properties [47]. All these results make the proposed microwire-composite a truly multi-functional composite for potentially a range of engineering applications.

#### Acknowledgements

F.X.Q is supported through Overseas Research Students Awards Scheme and University of Bristol Postgraduate Student Scholar-

ship. F.X.Q also wishes to thank the National Institute for Materials Science where part of the work was performed under NIMS Internship Program. H.X.P would like to acknowledge the financial support from the Engineering and Physical Science Research Council (EPSRC) UK under the Grant No. EP/F03850X.

#### References

- [1] Torquato S, Hyun S, Donev A. Multifunctional composites: optimizing microstructures for simultaneous transport of heat and electricity. *Phys Rev Lett* 2002;89(26):266601.
- [2] Thomas JP, Qidwai MA. Mechanical design and performance of composite multifunctional materials. *Acta Mater* 2004;52(8):2155–64.
- [3] Panina LV. Asymmetrical giant magneto-impedance (AGMI) in amorphous wires. *J Magn Magn Mater* 2002;249(1–2):278–87.
- [4] Panina LV, Mohri K, Uchiyama T, Noda M, Bushida K. Giant magneto-impedance in Co-rich amorphous wires and films. *IEEE Trans Magn* 1995;31(2):1249–60.
- [5] Makhovskiy DP, Panina LV, Mapps DJ. Field-dependent surface impedance tensor in amorphous wires with two types of magnetic anisotropy: helical and circumferential. *Phys Rev B* 2001;63(14):144424.
- [6] Phan M-H, Peng H-X. Giant magnetoimpedance materials: fundamentals and applications. *Prog Mater Sci* 2008;53(2):323–420.
- [7] Yelon A, Menard D, Britel M, Ciureanu P. Calculations of giant magnetoimpedance and of ferromagnetic resonance response are rigorously equivalent. *Appl Phys Lett* 1996;69(20):3084–5.
- [8] Sandacci SI, Makhovskiy DP, Panina LV. Valve-like behavior of the magnetoimpedance in the GHz range. *J Magn Magn Mater* 2004;272–276(part 3):1855–7.
- [9] Panina LV, Mohri K. Magneto-impedance effect in amorphous wires. *Appl Phys Lett* 1994;65(9):1189–91.
- [10] Alves F, Rached LA, Moutoussamy J, Coillot C. Trilayer GMI sensors based on fast stress-annealing of FeSiBCuNb ribbons. *Sens Actuators A* 2008;142(2):459–63.
- [11] Radu D, Astefanoaei I, Chiriac H. Temperature distribution in dc Joule-heated amorphous ribbons. *Phys Status Solidi A* 2005;202(13):2419–35.
- [12] da Silva FCS, Knobel M, Ferrari EF, Denardin JC, Miranda MGM, Bracho GJ, et al. Development of granular structure in Cu90Co10 ribbons through furnace and current annealing. *IEEE Trans Magn* 2000;36(5):3041–3.
- [13] Franco CS, Ribas GP, Bruno AC. Influence of the anisotropy axis direction and ribbon geometry on the giant magnetoimpedance of Metglas(R) 2705M. *Sens Actuators A* 2006;132(1):85–9.
- [14] Arcas J, Gomez-Polo C, Zhukov A, Vazquez M, Larin V, Hernando A. Magnetic properties of amorphous and devitrified FeSiBCuNb glass-coated microwires. *Nanostruct Mater* 1996;7(8):823–34.
- [15] Marin P, Vazquez M, Arcas J, Hernando A. Thermal dependence of magnetic properties in nanocrystalline FeSiBCuNb wires and microwires. *J Magn Magn Mater* 1999;203(1–3):6–11.
- [16] Vazquez M. Soft magnetic wires. *Phys B: Condens Matter* 2001;299(3–4):302–13.
- [17] Zhukov A, Zhukova V, Blanco JM, Cobeno AF, Vazquez M, Gonzalez J. Magnetostriction in glass-coated magnetic microwires. *J Magn Magn Mater* 2003;258–259:151–7.
- [18] Qin FX, Peng HX, Phan MH. Influence of varying metal-to-glass ratio on GMI effect in amorphous glass-coated microwires. *Solid State Commun* 2010;150(1–2):114–7.
- [19] Li XP, Zhao ZJ, Chua C, Seet HL, Lu L. Enhancement of giant magnetoimpedance effect of electroplated NiFe/Cu composite wires by dc Joule annealing. *J Appl Phys* 2003;94(12):7626–30.
- [20] Buznikov NA, Antonov AS, Granovsky AB, Kim CG, Kim CO, Li XP, et al. Current distribution and giant magnetoimpedance in composite wires with helical magnetic anisotropy. *J Magn Magn Mater* 2006;296(2):77–88.
- [21] Morikawa T, Nishibe Y, Yamadera H, Nonomura Y, Takeuchi M, Sakata J, et al. Enhancement of giant magneto-impedance in layered film by insulator separation. *IEEE Trans Magn* 1996;32(5):4965–7.
- [22] Correa MA, Bohn F, Viegas ADC, Carara MA, Schelp LF, Sommer RL. Giant magnetoimpedance in FM/SiO<sub>2</sub>/Cu/SiO<sub>2</sub>/FM films at GHz frequencies. *J Magn Magn Mater* 2008;320(14):E25–8.
- [23] García-Arribas A, Barandiarán JM, de Cos D. Finite element method calculations of GMI in thin films and sandwiched structures: size and edge effects. *J Magn Magn Mater* 2008;320(14):e4–7.
- [24] Taylor GF. A method of drawing metallic filaments and a discussion of their properties and uses. *Phys Rev* 1924;23(5):655–60.
- [25] Ulitovsky AV, Maianki IM, Avramenco AI. Method of continuous casting of glass coated microwire. Patent No 128427 (USSR), 150560, Bulletin no. 10, p. 14.
- [26] Peng HX, Qin FX, Phan MH, Tang J, Panina LV, Ipatov M, et al. Co-based magnetic microwire and field-tunable multifunctional macro-composites. *J Non-Cryst Solids* 2009;355(24–27):1380–6.
- [27] Pal SK, Manik NB, Mitra A. Dependence of frequency and amplitude of the ac current on the GMI properties of Co based amorphous wires. *Mater Sci Eng A* 2006;415(1–2):195–201.
- [28] Haddad YM. Advanced multilayered and fibre-reinforced composites. Kluwer Academic Publishers; 1998.

- [29] Velázquez J, Vázquez M, Zhukov AP. Magnetoelastic anisotropy distribution in glass-coated microwires. *J Mater Res* 1996;11(10):2499–505.
- [30] Chiriac H, Ovari TA, Pop G, Barariu F. Internal stresses in highly magnetostrictive glass-covered amorphous wires. *J Magn Magn Mater* 1996;160:237–8.
- [31] Tannous C, Gieraltowski J. Giant magneto-impedance and its applications. *J Mater Sci – Mater Electron* 2004;15(3):125–33.
- [32] Ryu GH, Yu SC, Kim CG, Yoon SS. Evaluation of anisotropy field in amorphous Fe<sub>71</sub>xNb<sub>7</sub>B<sub>22</sub>–x alloys by GMI measurement. *J Magn Magn Mater* 2000;215–216:359–61.
- [33] Qin FX, Pankratov N, Peng HX, Tang J, Panina LV. Influence of geometry on GMI effect of Co-based magnetic composite microwires. ICCM17. Edinburgh; 2009.
- [34] Velázquez J, García C, Vázquez M, Hernando A. Dynamic magnetostatic interaction between amorphous ferromagnetic wires. *Phys Rev B* 1996;54(14):9903.
- [35] Landau LD, Lifshitz EM. *Electrodynamics of continuous media: course of theoretical physics – Pergamon international library of science, technology, engineering and social studies*, Oxford: Pergamon Press, 1975, 4th rev.engl.ed.; 1975.
- [36] Garcia-Miquel H, Esbri MJ, Andres JM, Garcia JM, Garcia-Beneytez JM, Vazquez M. Power absorption and ferromagnetic resonance in Co-rich metallic glasses. *IEEE Trans Magn* 2001;37(1):561–4.
- [37] Antonov AS et al. Residual quenching stresses in glass-coated amorphous ferromagnetic microwires. *J Phys D Appl Phys* 2000;33(10):1161.
- [38] Aranda GR, Usov NA, Zhukova V, Zhukov A, Gonzalez J. Magnetostatic properties of Co-rich amorphous microwires: theory and experiment. *Phys Status Solidi A* 2008;205(8):1800–4.
- [39] Torcunov AV, Baranov SA, Larin VS. The internal stresses dependence of the magnetic properties of cast amorphous microwires covered with glass insulation. *J Magn Magn Mater* 1999;196–197:835–6.
- [40] Zuberek R, Szymczak H, Gutowski M, Zhukov A, Zhukova V, Usov NA, et al. Internal stress influence on FMR in amorphous glass-coated microwires. *J Magn Magn Mater* 2007;316(2):e890–2.
- [41] García-Miquel H, Carbonell J, Boria VE, Sánchez-Dehesa J. Experimental evidence of left handed transmission through arrays of ferromagnetic microwires. *Appl Phys Lett* 2009;94:054103.
- [42] Matsuzaki R, Melnykowycz M, Todoroki A. Antenna/sensor multifunctional composites for the wireless detection of damage. *Compos Sci Technol* 2009;69(15–16):2507–13.
- [43] Melik R, Unal E, Perkgoz NK, Puttlitz C, Demir HV. Metamaterial-based wireless strain sensors. *Appl Phys Lett* 2009;95(1):011106.
- [44] Sakai K, Asano N, Wada Y, Yoshikado S. Composite electromagnetic wave absorber made of soft magnetic material and polystyrene resin and control of permeability and permittivity. *J Eur Ceram Soc* 2010;30(2):347–53.
- [45] Xu X, Qing A, Gan YB, Feng YP. An experimental study on electromagnetic properties of random fibre composite materials. *Microw Opt Technol Lett* 2007;49(1):185–90.
- [46] Fernando GF, Degamber B. Process monitoring of fibre reinforced composites using optical fibre sensors. *Int Mater Rev* 2006;51(2):65–106.
- [47] Qin FX, Peng HX, Pankratov N, Phan MH, Panina LV, Ipatov M, et al. Exceptional EMI shielding properties of ferromagnetic microwires enabled polymer composites. *J Appl Phys* 2010;108:044510.